Vanadate Family as Spin-Gap Systems

Yutaka Ueda

Materials Design and Characterization Laboratory, Institute for Solid State Physics, University of Tokyo, Roppongi 7-22-1, Minato-ku, Tokyo 106-8666, Japan

Received March 31, 1998. Revised Manuscript Received June 30, 1998

The structural and magnetic properties of the vanadate family with the chemical formula AV_2O_5 (A = Li, Na, Cs, Mg, and Ca) are reviewed in terms of low-dimensional quantum-spin systems. These compounds have layered structures with A cations lying between layers. A structural element common to them is a VO_5 square pyramid formed by five oxygens surrounding the V ion. Each compound has a structure with a characteristic arrangement of VO_5 square pyramids formed by the sharing of edges and/or corners. All of these compounds are low-dimensional, spin-1/2 magnets and are spin-gap systems except γ-LiV_2O_5. α'-NaV_2O_5 is a spin-Peierls system with the transition temperature $T_{SP} = 35$ K and the energy gap $\Delta = 114$ K. The parameter $2\Delta/k_BT_{SP} = 3.53$ holds well for the all organic and inorganic spin-Peierls compounds except α'-NaV_2O_5 for which the measure is 6.44. This difference suggests that the transition observed in α'-NaV_2O_5 is not a conventional spin-Peierls transition but an exotic one. Both MgV_2O_5 and CaV_2O_5 are spin-ladder systems with a similar two-leg ladder structure but the gap energy (∼17 K) observed in MgV_2O_5 is very small compared with that (∼600 K) in CaV_2O_5. CsV_2O_5 is a dimer system with a spin gap of ∼160 K. γ-LiV_2O_5, which has one-dimensional zigzag chains in the structure, shows neither spin gap nor magnetic order down to 0.5 K.

Contents

There exist many kinds of vanadium oxides that have manifested a variety of structural and electromagnetic properties. One of the most remarkable features is the metal−insulator transition in the binary vanadium oxides.[1] These vanadium oxides had been the core materials in the study of the highly correlated electronic system until the discovery of the high-temperature-superconducting cuprates. In these vanadium oxides, vanadium ions have various kinds of oxygen coordination, for example, octahedral, tetrahedral, trigonal, and square pyramidal, etc. A typical vanadium oxide with a square pyramidal coordination is V_2O_5. It has a layer structure, and the layers are formed by sharing the edges and/or corners of square pyramids VO_5. The vanadium ions are inside the square pyramids. V_2O_5 can intercalate various kinds of ions between the layers. $A_xV_2O_5$ with alkaline- or alkaline-earth-metal ions as intercalants (A) has been well known as vanadium oxide bronzes.

The compounds AV_2O_5 (A = Li, Na, Cs, Mg and Ca) are situated as end members of such vanadium oxide bronzes. The sites between the layers in AV_2O_5 are fully occupied by A ions. A structural element common to these vanadium oxides is a VO_5 square pyramid, and each compound has a characteristic intralayer structure formed by sharing the edges and corners of VO_5 square pyramids. With the arrangements of the magnetic V^{4+} ion (d^1, $S = 1/2$), these compounds have unique structures as low-dimensional magnets; for examples, one-dimensional (1-D) chain, zigzag chain, ladder, and dimer.

Low-dimensional spin systems with $S = 1/2$ and a singlet ground state are of great interest because of their fundamental quantum nature. These systems have been discovered mainly in copper and nickel compounds. Recent studies have been focused on the cuprates, like, for example, $CuGeO_3$[2] for the spin-Peierls system and $SrCu_2O_3$[3] for the two-leg ladder system. Since the discovery of spin-gap in CaV_4O_9,[4] which is the first realization of a two-dimensional spin-plaquette system, compounds of the vanadate family containing VO_5 pyramids have been drawing experimentalists' attention to low-dimensional magnetic systems with $S = 1/2$ V^{4+} ions. The vanadium oxides AV_2O_5 have also been extensively studied and have shown various kinds of quantum spin phenomena, such as spin-Peierls transition and spin-gap in the ladder structure. In this article, the structural and magnetic properties of AV_2O_5 (A = Li, Na, Cs, Mg, and Ca) are reviewed in terms of a low-dimensional quantum-spin system.

α'-NaV_2O_5 (Spin-Peiels System)

α'-NaV_2O_5 crystallizes in an orthorhombic cell with the space group $P2_1mn$.[5] The schematic crystal struc-

10.1021/cm980215w CCC: $15.00 © 1998 American Chemical Society
Published on Web 10/02/1998

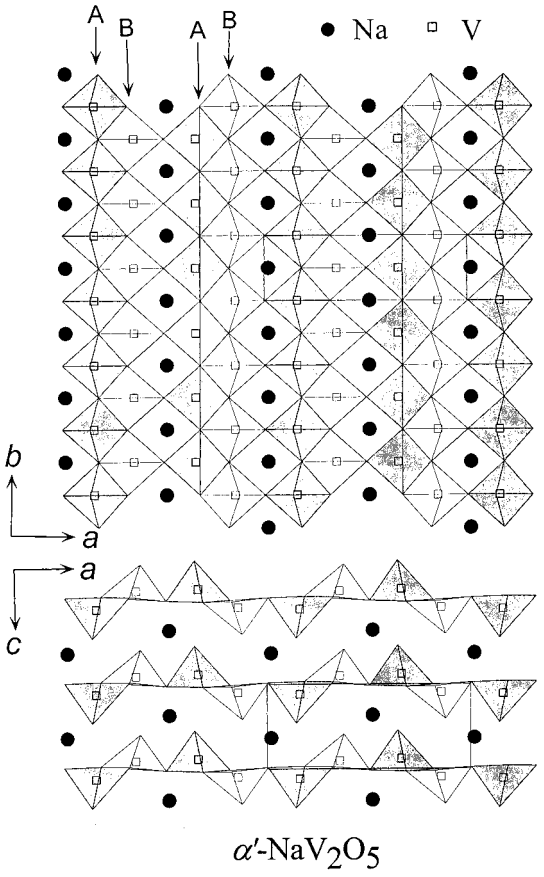

Figure 1. Schematic crystal structure of orthorhombic α′-NaV_2O_5. A and B represent the $V^{4+}O_5$ and $V^{5+}O_5$ chains, respectively.

ture of α′-NaV_2O_5 is shown in Figure 1. It consists of layers of VO_5 square pyramids that share edges and corners, and sodium ions lying between the layers. There are two crystallographic vanadium sites, which form two kinds of VO_5 chain (A and B in Figure 1) along the *b*-axis. From the fact that α′-NaV_2O_5 is a mixed-valence ($V^{4+}/V^{5+} = 1$) oxide and the analysis of the V−O bond length and Na−V distance, it has been considered that the A and B chains are possibly $V^{4+}O_5$ and $V^{5+}O_5$ chains, respectively.[5] In this structure, α′-NaV_2O_5 is expected to be a quasi-1-D spin system because the magnetic $V^{4+}O_5$ chains are isolated by the nonmagnetic $V^{5+}O_5$ chains. Actually, the magnetic susceptibility for powder samples shows a typical temperature dependence for a 1-D magnetic system, as shown in Figure 2. The magnetic susceptibility can be excellently fitted with the Bonner−Fisher curve[7] with $J/k_B = 560$K and $g = 2$, where J, k_B, and g are the exchange constant, the Boltzmann constant, and the powder-averaged *g*-factor, respectively.[6] Furthermore, the magnetic susceptibility rapidly decreases below 35 K with decreasing temperature, showing a slight upturn below 12 K. The magnetic susceptibilities along the *a*-, *b*-, and *c*-axes, measured with a single crystal, show sharp and isotropic reduction of magnetic susceptibility below 35 K, as shown in Figure 3. These results suggest that the transition is not a magnetic transition but a spin-Peierls transition.[8]

The spin-Peierls transition is one of the most interesting phenomena observed in low-dimensional quantum-spin systems. It occurs in crystals containing linear (1-D) chains of spin-1/2 ions coupled by the antiferromagnetic exchange interaction. Below a spin-Peierls transition temperature T_{SP}, the structure of the underlying lattice changes so that the chains become dimerized. The dimerization in turn implies that the magnetic exchange interaction alternates in magnitude along the chain. The mechanism of the spin-Peierls instability is the coupling of the lattice phonons to the spins. Below T_{SP}, the ground state is a nonmagnetic spin singlet, and a finite energy gap opens in the excitation spectrum. The spin-Peierls transition has been observed in organic compounds[9−12] and later in the inorganic metal oxide $CuGeO_3$.[2]

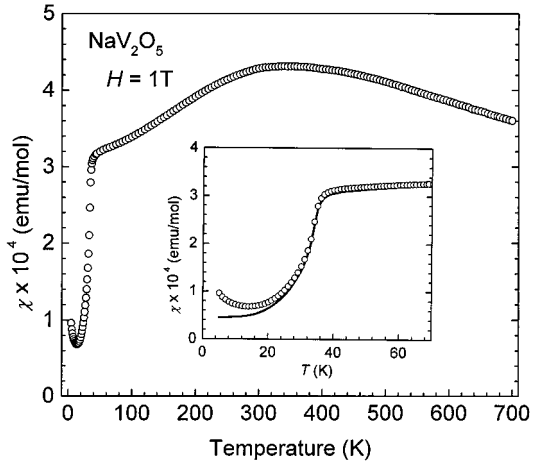

Figure 2. Temperature dependence of magnetic susceptibility of α′-NaV_2O_5. The solid line in the inset shows the susceptibility derived by subtracting the Curie contribution.

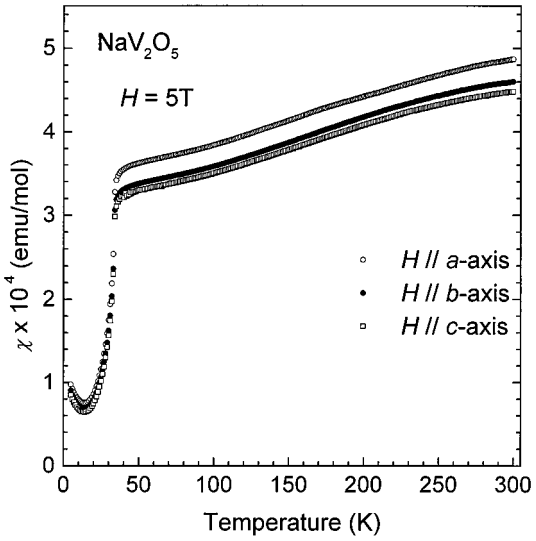

Figure 3. Temperature dependence of magnetic susceptibility along *a*-, *b*-, and *c*-axes in a single crystal of α′-NaV_2O_5.

A spin-singlet ground state in α′-NaV_2O_5 has been confirmed by nuclear magnetic resonance (NMR),[13] and the lattice dimerization and spin-gap formation below 35 K have been observed in X-ray and neutron scattering measurements.[14,15] A single-crystal X-ray scattering experiment shows superlattice reflections with a lattice modulation vector $\boldsymbol{q} = (1/2, 1/2, 1/4)$.[14] The doubling of a unit cell along the *b*-axis implies lattice dimerization along the V^{4+} chains. The unit cell is also doubled along the *a*-axis, which intrinsically contains two V^{4+} chains. This situation is very similar to the case of $CuGeO_3$ in

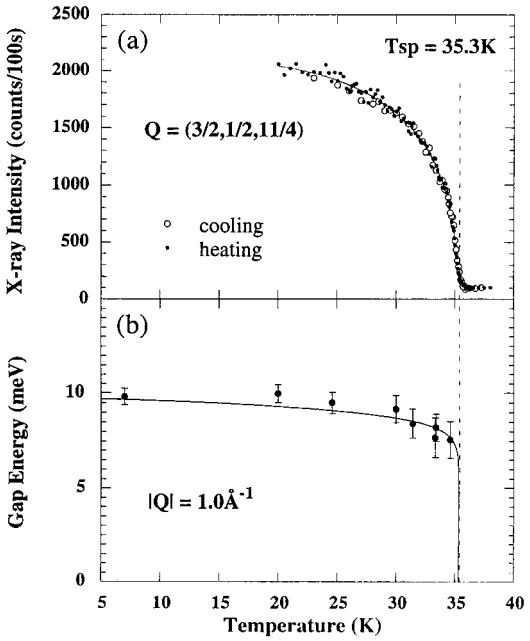

Figure 4. Temperature dependence of (a) the superlattice intensity measured at $\boldsymbol{Q}$ = (3/2, 1/2, 11/4) using X-ray scattering and (b) the gap energy Δ measured at $|\boldsymbol{Q}|$ = 1.0 Å^{-1} using neutron scattering in α′-NaV_2O_5 (ref 14). The curves are guides for the eye.

Table 1. Various Parameters of Spin-Peierls Systems

systems	J/k_B (K)	Δ (K)	T_{SP} (K)	$2\Delta/k_BT_{SP}$
TTF−CuBDT[9]	77	21	12	3.50
TTF−AuBDT[10]	68	3.7	2	3.70
MEM-$(TCNQ)_2$[11]	106	28	18	3.11
SBTTF-$TCNQCl_2$[12]	160	67	38	3.52
$CuGeO_3$[2]	121	24.5	14	3.50
α'-NaV_2O_5	560	114	35.3	6.44

which a unit cell is also doubled along the *b*-axis containing two Cu^{2+} chains aligned perpendicular to the chain direction along the *c*-axis.[16−18] It is surprising that the unit cell quadruples in size along the *c*-axis, which is the stacking direction of the layers of the VO_5 pyramids connected two-dimensionally. The atomic displacement pattern, that is the crystal structure of the spin-Peierls phase, has not been solved. Figure 4 shows the temperature dependence of the superlattice intensity measured at $\boldsymbol{Q}$ = (3/2, 1/2, 11/4) using X-ray scattering of the single crystal and the gap energy Δ at $|\boldsymbol{Q}|$ = 1.0 Å^{-1} using neutron scattering of the powder sample.[14] Neither discontinuous change in intensity nor appreciable thermal hysteresis has been observed, which indicates that this transition is of the second order. The spin-Peierls transition in α′-NaV_2O_5 has also been confirmed by electron spin resonance (ESR).[19] α′-NaV_2O_5 is the second inorganic spin-Peierls compound. The parameters of α′-NaV_2O_5 as the spin-Peierls system are shown in Table 1 together with those of another organic and inorganic spin-Peierls compounds. It is notable that the theoretically driven BCS-type formula in a weak coupling regime for the spin-Peierls transition,[20] $2\Delta/k_BT_{SP}$ = 3.53, holds well for the all-organic and inorganic spin-Peierls compounds except α′-NaV_2O_5, for which the measure is 6.44. This exceptionally large value means that the transition observed in α′-NaV_2O_5 is not a conventional spin-Peierls transition but an exotic one. Anomalous behaviors that cannot be explained on the basis of simple 1-D spin-Peierls chains have been observed in the structure,[14] NMR,[21] thermal conductivity,[22] and dielectric constant[23] measurements. In the connection with these anomalous behaviors, there are some arguments[24] that the crystal structure at room temperature is not a previously reported $P2_1mn$ in the space group but a *Pmmn*. The latter space group is identical with that for V_2O_5 and implies the presence of only one kind of V sites in contrast to two V sites in $P2_1mn$. From these results, a possibility of charge ordering or charge disproportionation has been discussed for the transition in α′-NaV_2O_5. A detailed mechanism of the transition has been an open question.

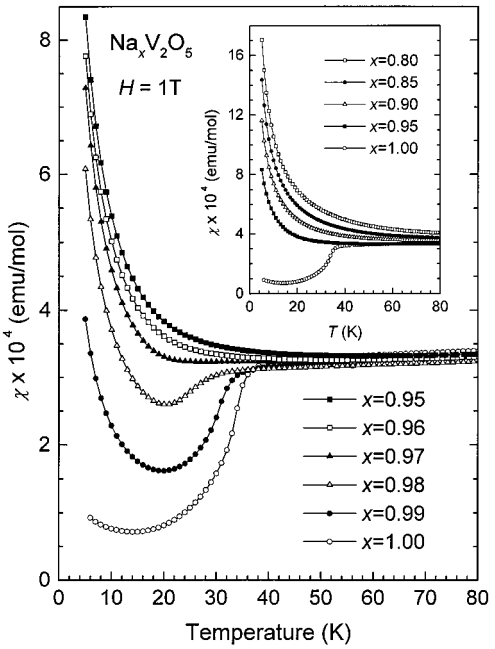

Figure 5. Temperature dependence of magnetic susceptibility of α′-$Na_xV_2O_5$ ($0.80 \le x \le 1.00$).

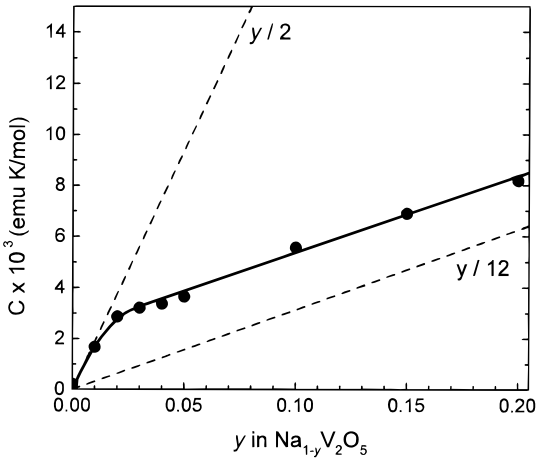

Figure 6. Compositional dependence of Curie constant in α′-$Na_{1-y}V_2O_5$. The Curie constant was obtained from fitting the magnetic susceptibility to the Curie−Weiss law between 5 and 15 K. The dependence changes from the *y*/2 to *y*/12 around *y* = 0.03 where the spin-Peierls transition disappears.

α′-NaV_2O_5 has a rather wide region of Na deficiency ($0.8 \le x \le 1.0$ in α′-$Na_xV_2O_5$).[25] The spin-Peierls transition is suppressed by Na deficiency and vanishes around α′-$Na_{0.97}V_2O_5$.[25] Figure 5 shows the magnetic susceptibility of the powdered α′-$Na_xV_2O_5$ below 80 K. Sodium deficiency introduces nonmagnetic V^{5+} ions in

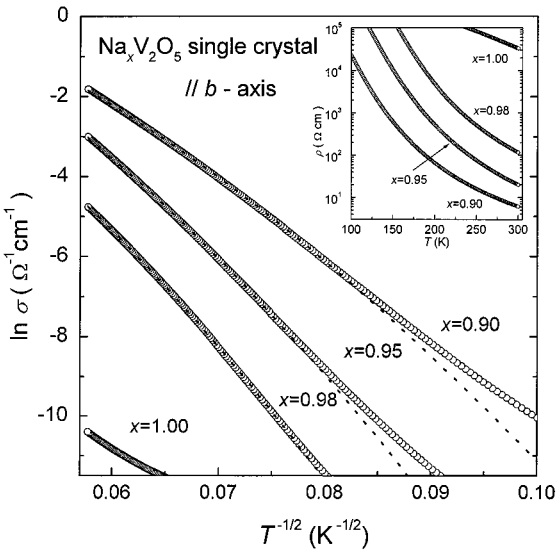

Figure 7. Logarithm of the electric resistivity versus $1/T^{-1/2}$ of α′-$Na_xV_2O_5$. The inset shows the resistivity of α′-$Na_xV_2O_5$ as a linear function of temperature. The resistivity is measured along *b*-axis parallel to the 1-D chains using single crystals.

the magnetic V^{4+} linear chains and cuts the chains. A Curie-like increase of magnetic susceptibility that is proportional to Na-deficiency has been observed in α′-$Na_xV_2O_5$ at low temperature, as shown in Figure 5. Evidence for a magnetic order, however, has not been observed in contrast to the Zn-doped $CuGeO_3$[26−28] or $SrCu_2O_3$.[29] This result indicates that α′-NaV_2O_5 is an ideal 1-D magnetic system and the magnetic interchain interaction is very weak. The Curie constants obtained from fitting the magnetic susceptibility to Curie−Weiss laws between 5 and 15 K are shown in Figure 6 as a function of *y* in α′-$Na_{1-y}V_2O_5$.[25] In this fitting, the Weiss temperatures obtained were ∼0 K to ∼ −0.9 K in all samples. The dotted lines in Figure 6 represent the *y*/2 and *y*/12 dependence, assuming free ions with $S = 1/2$ associated with Na deficiency. At first, the Curie constant increases with a proportion of *y*/2 and then *y*/12 above $y = 0.03$. The turning point of $y = 0.03$ corresponds to the composition where the spin-Peierls transition disappears. The introduction of a nonmagnetic ion into a magnetic linear chain affects the magnetic properties in a different manner in the spin-Peierls state and the 1-D magnetic uniform state, respectively. Such effects may be more remarkable in the state with a spin-gap than in the 1-D magnetic uniform state. Some theories predict that the compositional dependence of the Curie constant lies between *y*/4 and *y*/12 in the spin-ladder system with the spin gap.[30,31]

The stoichiometric α′-NaV_2O_5 is semiconductive. With Na deficiency, α′-$Na_xV_2O_5$ becomes conductive but remains semiconductive. The electric resistivities of α′-$Na_xV_2O_5$ measured along the *b*-axis (the linear chain direction) using single crystals are shown in Figure 7.[25] The temperature dependence of resistivity does not obey any activation type but shows a $T^{-1/2}$ dependence, as shown in Figure 7. This dependence seems to be consistent with a variable range hopping in the 1-D system. This result suggests that the carriers are doped into the 1-D chain by Na deficiency but do not induce clean metallic behavior because an arbitrary small concentration of defects often leads to localization in a 1-D material. This point is significant, differing from the doping effect in $CuGeO_3$ and $SrCu_2O_3$, where the doping or substitution of other cations for Cu has not resulted in the carrier doping but a long-range antiferromagnetic order.

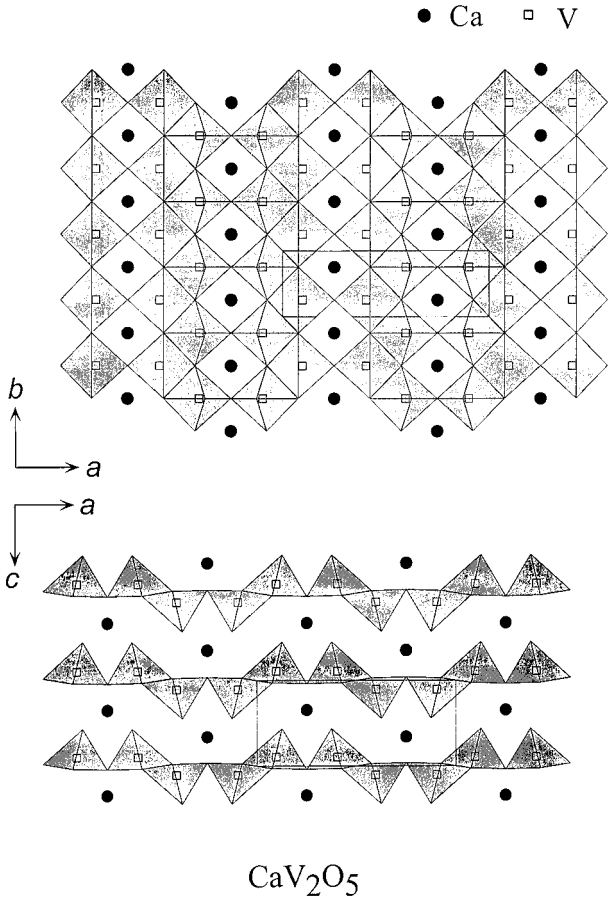

Figure 8. Schematic crystal structure of orthorhombic CaV_2O_5.

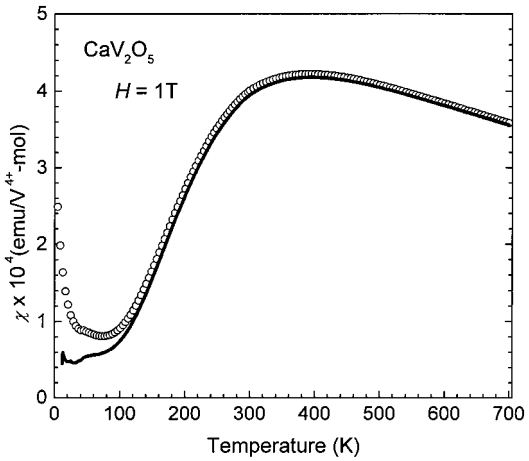

Figure 9. Temperature dependence of magnetic susceptibility of CaV_2O_5. The solid line shows the susceptibility derived by subtracting the Curie contribution from impurities.

CaV_2O_5 (Spin-Ladder System with a Spin Gap)

The structure of CaV_2O_5 is orthorhombic, belongs to the space group *Pmmn*,[32] which is identical to that of V_2O_5, and consists of layers of VO_5 pyramids with Ca ions located between these layers, as shown in Figure 8. CaV_2O_5 has a similar intralayer structure to that of

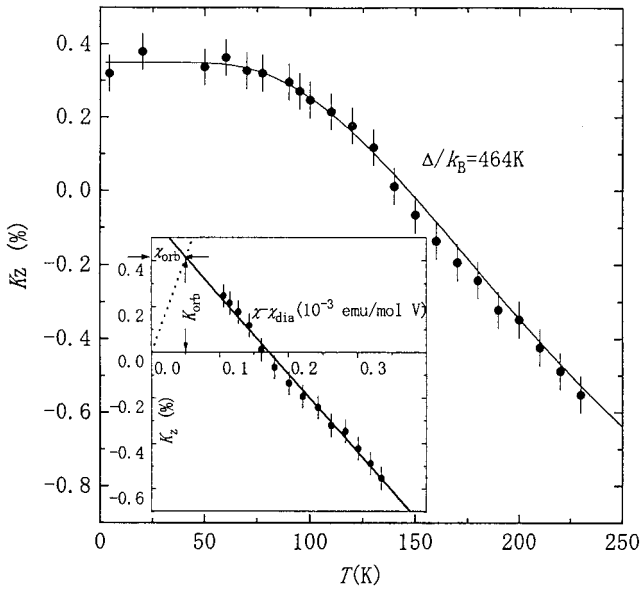

Figure 10. Temperature dependence of the *z*-component of the ^{51}V Knight shift (K_z) in CaV_2O_5 (ref 34). The solid line represents the values calculated using $\Delta/k_B = 464$K and $K_{z,orb} = 0.36\%$ in terms of the ladder model. The inset shows $K - \chi$ plot with temperature ranging from 100 to 230 K.

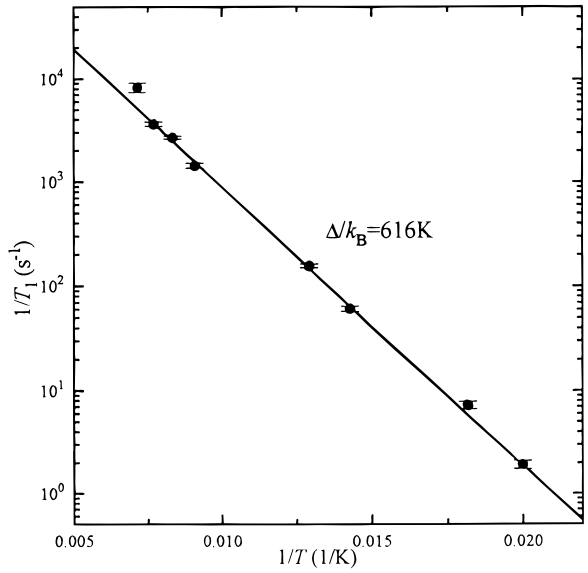

Figure 11. Temperature dependence of spin−lattice relaxation rate ($1/T_1$) observed by ^{51}V NMR in CaV_2O_5 (ref 34). The solid line represents the theoretically predicted values.

α′-NaV_2O_5, but it is a monovalent oxide different from α′-NaV_2O_5, and all vanadium ions are magnetic tetravalent V^{4+} ions in CaV_2O_5. The structure viewed along the *c*-axis is very similar to that of two-leg ladder cuprate $SrCu_2O_3$[3] and therefore the basic structure of CaV_2O_5 can be considered in two ways in terms of the exchange couplings. One is a ladder structure formed by the exchange coupling through the corners of the VO_5 pyramids. The other is a zigzag chain system, which is due to the exchange coupling across the edges of the VO_5 pyramids. Because the spins along the zigzag chain can be considered to be geometrically frustrated, a two-leg spin-ladder is a plausible spin system for CaV_2O_5. An energy gap originating from the inherent topological structure with $S = 1/2$ for a two-leg ladder structure has been theoretically understood and then actually the formation of the spin singlet ground state without lattice distortion has been observed in the first two-leg ladder compound $SrCu_2O_3$.[3,33]

Figure 9 shows the raw data of magnetic susceptibility. The solid line in Figure 9 is the magnetic susceptibility derived by subtracting the contribution of impurities. The magnetic susceptibility has a maximum around 400 K, decreases with decreasing temperature, and reaches a small constant value below ∼70 K. This behavior is a typical low-dimensional magnetic one. The spin-singlet ground state was directly confirmed by ^{51}V NMR.[34] Figure 10 shows the temperature dependence of the *z*-component of the Knight shift (K_z). The parameter K_z increases with decreasing temperature, reflecting the decrease of the local spin susceptibility, and below 70 K it reaches a constant value of ∼0.3%, which is a typical value for a spin-singlet V^{4+} state. The *x* and *y* components of the Knight shift or *K* ($K_x = 0.3\%$, $K_y = 0.17\%$) do not change within the experimental error. The existence of an energy gap Δ between nonmagnetic ground state and magnetic excited states was also confirmed from an activation type behavior of the spin−lattice relaxation rate ($1/T_1$), as shown in Figure 11.

According to the ladder model, the *d*-spin susceptibility (χ_{spin}) and $1/T_1$ are expressed as[35]

$$\chi_{spin} \propto T^{-1/2} \exp(-\Delta/k_B T)$$

$$1/T_1 \propto \exp(-\Delta/k_B T)\,[0.80908 - \ln(\omega_0/T)]$$

where ω_0 is the nuclear resonance frequency. The fit of the experimental data for K_z and $1/T_1$ to the relations just presented, using the relation $K_{z,spin} \propto \chi_{spin}$, where $K_z = K_{z,spin} + K_{z,orb}$ is quite good, and the values of Δ/k_B obtained from $K_{z,spin}$ and $1/T_1$ are 464 and 616 K, respectively. Because the exchange interaction can be estimated to be ∼600 K, the observed energy gap is much larger than the theoretical value of $\Delta \approx J/2 \approx 300$ K in the ladder limit. There are some arguments that CaV_2O_5 is significantly closer to the dimer limit with a large exchange interaction along the rung.[36]

In CaV_2O_5, V sites are substituted by nonmagnetic Ti^{4+} ions to the extent of ∼10%. Figure 12 shows the magnetic susceptibility of $Ca(V_{1-x}Ti_x)_2O_5$. The Curie-like increase of magnetic susceptibility at low temperature is enhanced by the substitution of Ti, but any anomaly for a magnetic order has not been observed in the susceptibility curves, which is in contrast to the Zn-doped $SrCu_2O_3$.[29]

MgV_2O_5 (Spin-Ladder System with a Spin Gap)

MgV_2O_5 is a tetravalent oxide like CaV_2O_5. Figure 13 shows the crystal structure of MgV_2O_5.[37] The crystal structure consists of layers formed by edge- and corner-shared $V^{4+}O_5$ square pyramids with magnesium ions between the layers. The orthorhombic MgV_2O_5 is very analogous to CaV_2O_5 in structure, but the manner of layer stacking is somewhat different from that in CaV_2O_5; that is, the layers in MgV_2O_5 are alternatively stacked with a shift by *b*/2 along [010]. This result implies a doubling of the *c* parameter compared with CaV_2O_5. Because MgV_2O_5 has an intralayer network of VO_5 square pyramids similar to that in CaV_2O_5, it is

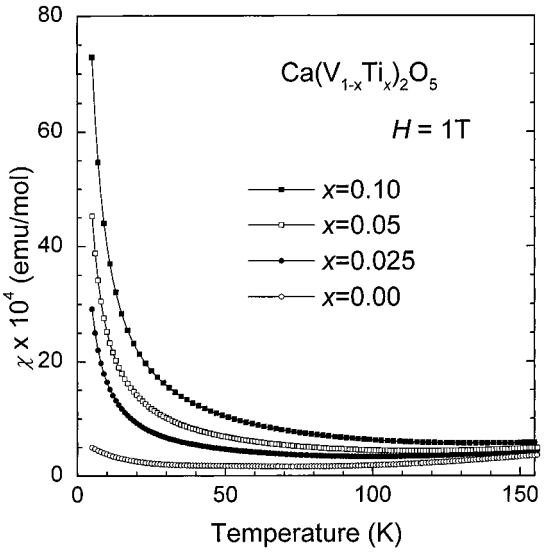

Figure 12. Temperature dependence of magnetic susceptibility of $Ca(V_{1-x}Ti_x)_2O_5$ ($0.00 \leq x \leq 0.10$).

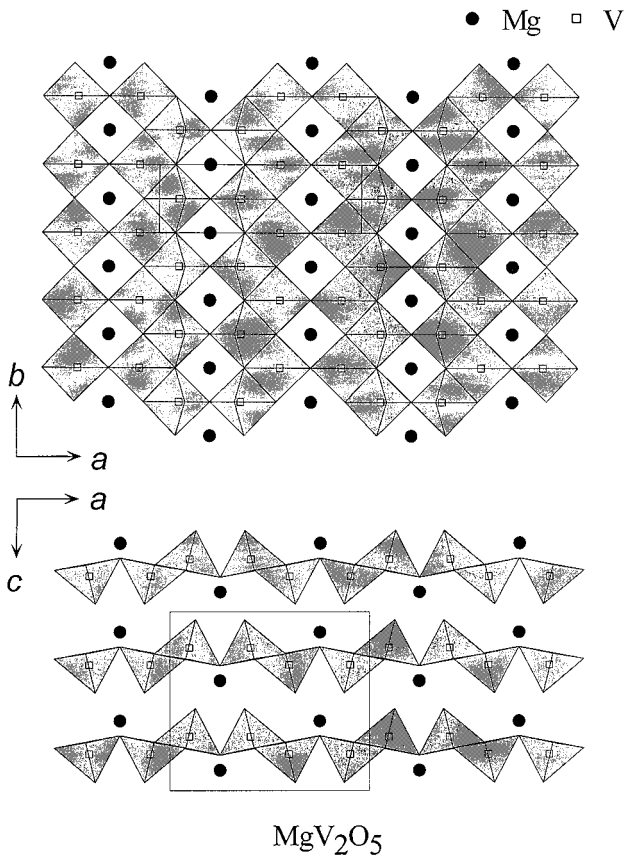

Figure 13. Schematic crystal structure of orthorhombic MgV_2O_5.

very interesting to determine whether MgV_2O_5 is a spin-ladder system with a spin gap.

Figure 14 shows the temperature dependence of the magnetic susceptibility of MgV_2O_5.[38] It has a characteristic of a low-dimensional magnetic system, that is, a broad maximum around 100 K. Below ~15 K, the magnetic susceptibility decreases more rapidly with decreasing temperature and shows a slight upturn below 5 K. This increase of magnetic susceptibility at low temperature may be due to magnetic impurities included accidentally. The magnetization curve up to

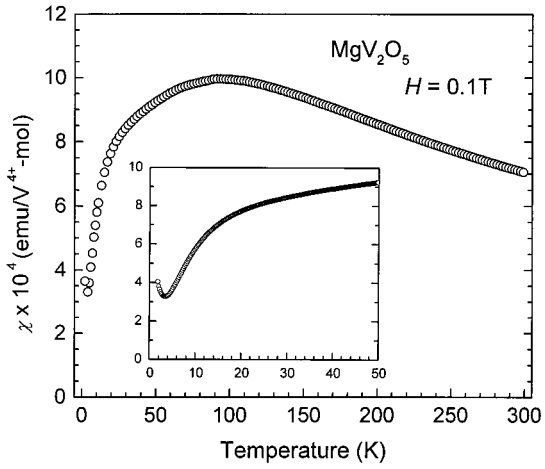

Figure 14. Temperature dependence of magnetic susceptibility of MgV_2O_5.

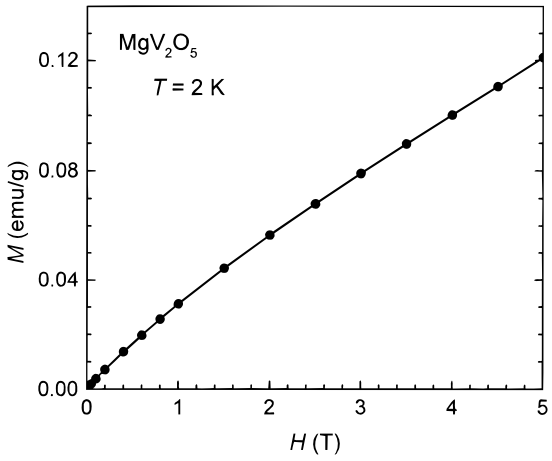

Figure 15. Magnetization curve of MgV_2O_5 in a field up to 5 T measured using a SQUID magnetometer.

5 T at 2 K, shown in Figure 15, consists of two components. One component is a paramagnetic one and has a tendency to saturate at high external field. The other component linearly increases with increasing magnetic field in the magnetization. The former can be considered to originate from magnetic impurities. The concentration of the magnetic impurities can be estimated from the saturated magnetization to be ~0.07% by assuming $S = 1/2$. The inflection of magnetic susceptibility around 15 K suggests a magnetic order, but the muon spin rotation (μSR) experiments have revealed no evidence for a magnetic order down to the lowest temperature (2.5 K).[39] An excitation peak at ~2 meV has been observed in the inelastic neutron spectra measured with powder samples, as shown in Figure 16.[40] The observed $\boldsymbol{Q}$-dependence of the intensity at constant energy transfer shows peaks around the positions corresponding to the so-called (π,π) and (3π,π), and the temperature dependence of the intensity can be well reproduced by a calculation assuming an excitation from singlet to triplet state.[40] These results strongly suggest a spin-singlet ground state in MgV_2O_5. Therefore, the linear component in the magnetization curve can be attributed to the orbital susceptibility (Van Vleck term), which can be estimated from the slope to be 2.2×10^{-4} emu/V^{4+}-mol. This value is rather large compared with those of spin-singlet states in other vanadium oxides.

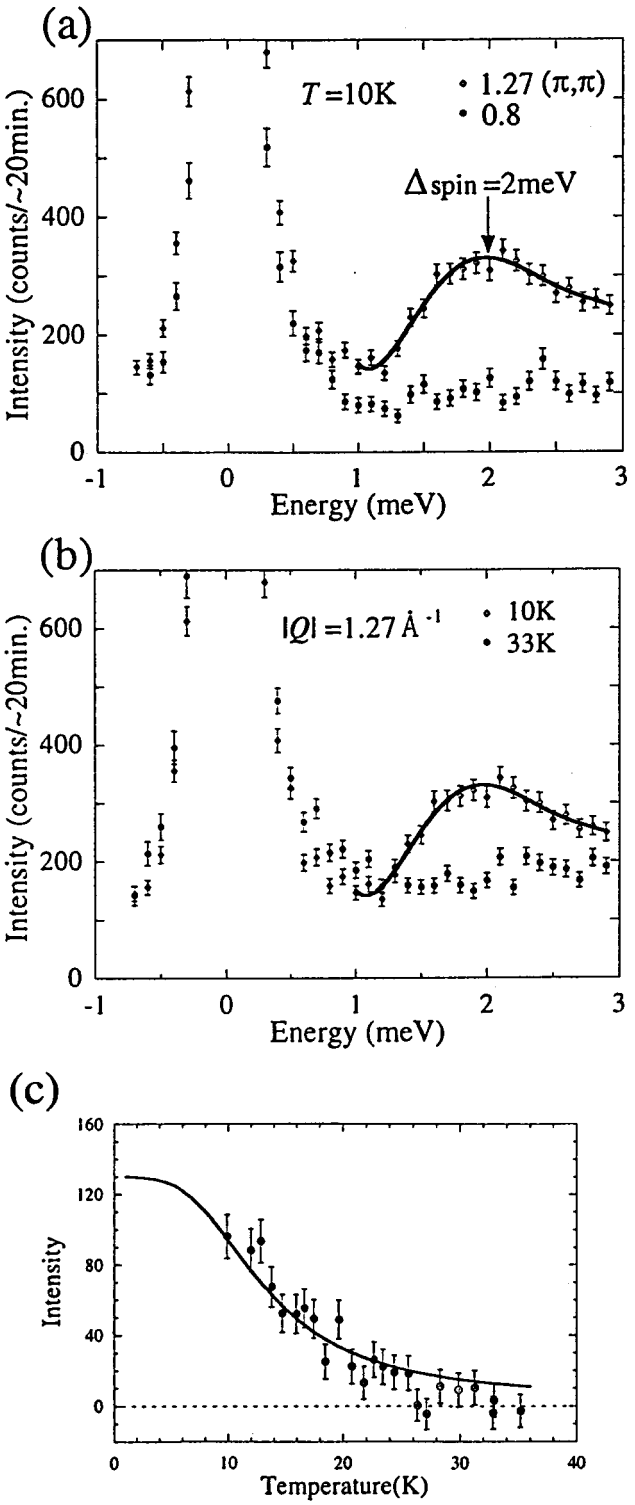

Figure 16. Typical neutron energy scans in powdered MgV_2O_5 (a) at $|\boldsymbol{Q}| = 1.27$ and 0.8 Å^{-1} at 10 K and (b) at $|\boldsymbol{Q}| = 1.27$ Å^{-1} at 10 and 33 K, and (c) temperature dependence of intensity of peak at 2 meV (ref 40).

Ohama et al.[13] pointed out that the magnetic susceptibility of the spin-Peierls state in α′-NaV_2O_5 is about twice as large as the temperature-independent term in the uniform state. Such large orbital susceptibilities may be a characteristic of the spin-singlet state of the V^{4+} ion with a pyramidal coordination of oxygen.

The spin-singlet ground state suggests that MgV_2O_5 is either a spin-Peierls system similar to α′-NaV_2O_5 or a two-leg spin-ladder system similar to CaV_2O_5. The possibility of spin-Peierls system may be ruled out from the structural characteristics, although the rapid decrease of magnetic susceptibility below 15 K is suggestive of a spin-Peierls transition. At present, there is no evidence of lattice distortion in the powder samples of MgV_2O_5. The small gap energy of ~2 meV observed in the neutron scattering experiments suggests the possibility of the observation of a field-induced transition to a gapless state in high fields. Figure 17 shows the magnetization curves measured in steady magnetic fields up to 17 T at 1.5 and 4.2 K.[38] The transition can be clearly seen at around $H_c \sim 12.5$ T in the magnetization curves at 1.5 and 1.7 K. The magnetization increases almost linearly up to 8 T and above 12.5 T it increases more steeply. At 4.2 K, the slope in the magnetization changes more gently around the critical field. It is considered that the level crossing between the singlet ground state and the excited triplet state occurs at a critical field H_c corresponding to the excitation gap at zero field, and that the system is in a gapless magnetic state with a finite magnetic susceptibility above H_c. The excitation gap between the ground state and the lowest excited triplet state in a magnetic field H can be expressed as $\Delta(H) = \Delta - g\mu_B H$, where Δ is the excitation gap at zero field and the Δ/k_B of MgV_2O_5 can be estimated from H_c to be ~17 K, which is in agreement with $\Delta/k_B \sim 20$ K from the neutron scattering studies. These results indicate that MgV_2O_5 is a spin-ladder system with a spin-gap of ~17 K. This very small value should be contrasted with the much larger value (~500 K) for CaV_2O_5.

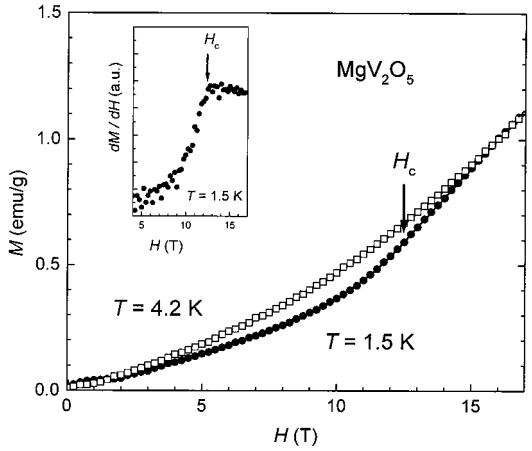

Figure 17. Magnetization curves of MgV_2O_5 measured in steady magnetic fields up to 17 T at 1.5 and 4.2 K. The inset shows the dM/dH versus H curve at 1.5 K.

γ-LiV_2O_5 (S = 1/2 Quasi-1-D System without Spin Gap)

The orthorhombic γ-LiV_2O_5 has a layer structure with lithium ions between the layers. In this structure there are two crystallographic vanadium sites that form two kinds of zigzag chains, the shaded and white zigzag chains in Figure 18. The valence states of vanadium ions were inferred from the results of structural analysis to be V^{4+} for the shaded zigzag chains and V^{5+} for the white zigzag chains.[41] Within the layers, $V^{4+}O_5$ (shaded) zigzag chains are linked to $V^{5+}O_5$ (white) zigzag chains by sharing corners, as shown in Figure 18. In the

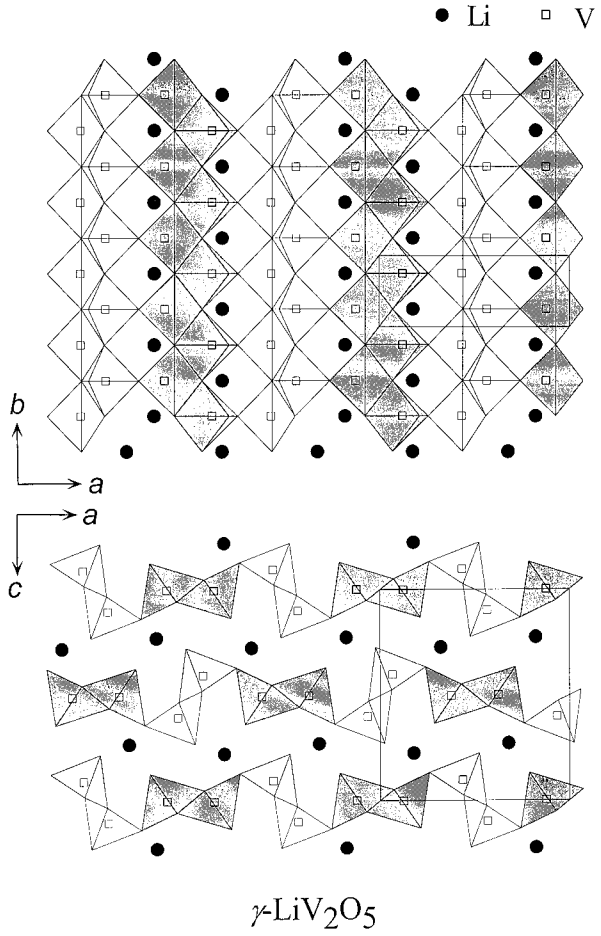

Figure 18. Schematic crystal structure of orthorhombic γ-LiV_2O_5. The dark and white VO_5 square pyramids represent $V^{4+}O_5$ and $V^{5+}O_5$ pyramids, respectively.

structure of γ-LiV_2O_5, there are two kinds of $V^{4+}O_5$ pyramids with apex oxygens above and below the sheet in Figure 18. Each kind of $V^{4+}O_5$ pyramid forms an infinite linear chain by sharing a corner with the same kind of pyramid or one kind of pyramid forms an infinite zigzag chain by sharing an edge with the other kind of pyramid. Therefore, the magnetic structure can be regarded as a double-linear chain system or a zigzag chain system. In either case, γ-LiV_2O_5 is expected to be a quasi-1-D-spin system because each double-linear chain or zigzag chain is isolated by the nonmagnetic $V^{5+}O_5$ double-linear or zigzag chains.

Figure 19 shows the temperature dependence of the magnetic susceptibility of γ-LiV_2O_5 measured in the powdered samples.[42] The magnetic susceptibility has a broad maximum at ~200 K and shows a good fit to the equations for a $S = 1/2$ 1-D Heisenberg antiferromagnetic linear chain model[7] with $J/k_B = 308$ K[42] and $g = 1.8$, as given by the solid line in Figure 19. These results are consistent with the characteristics of the crystal structure. The magnetic susceptibility extrapolated to the lowest temperature is much larger than that of Van Vleck paramagnetism of open shells of the V^{4+} ions, and any anomaly suggesting a magnetic order has not been observed in the susceptibility curve. It has been confirmed by ^{7}Li NMR that the ground state of γ-LiV_2O_5 is neither a spin-singlet state nor a magnetically ordered state down to 0.5 K.[43] γ-LiV_2O_5 is a typical 1-D magnet in which the interchain exchange interaction is very weak. Fujiwara et al.[43] have observed an anomalous behavior of spin−lattice relaxation rate that can be explained by considering the contribution from the staggered- and uniform-spin fluctuation.

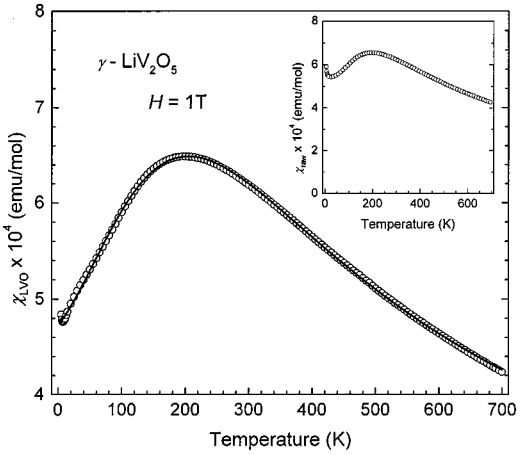

Figure 19. Temperature dependence of magnetic susceptibility of γ-LiV_2O_5. The solid line shows a fit to the equation for a $S = 1/2$ 1-D Heisenberg antiferromagnetic linear chain model with $J/k_B = 308$ K, $g = 1.8$.

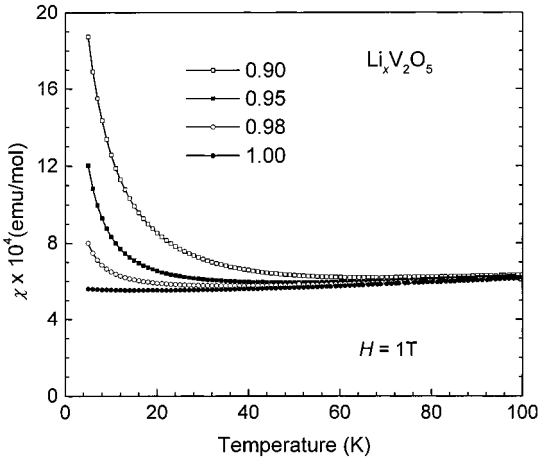

Figure 20. Temperature dependence of magnetic susceptibility of γ-$Li_xV_2O_5$ ($0.90 \leq x \leq 1.00$).

γ-LiV_2O_5 shows Li deficiency with somewhat narrower range compared with α'-$Na_xV_2O_5$. Figure 20 shows the magnetic susceptibility of the powdered γ-$Li_xV_2O_5$ below 100 K. Li deficiency introduces nonmagnetic V^{5+} ions in the magnetic V^{4+} linear chains and cuts the chains. A Curie-like increase of magnetic susceptibility is observed at low temperature, but any evidence for a magnetic order has not been observed. The Curie constant obtained from fitting the magnetic susceptibility to a Curie law between 5 and 15 K, assuming free ion with $S = 1/2$ associated with Li deficiency, increases with a proportion between $y/5$ and $y/6$ in γ-$Li_{1-y}V_2O_5$. The little dependence of Curie constant on the Li deficiency may also be caused from quantum effects, although γ-LiV_2O_5 is not a system with a spin gap. This result is consistent with that observed from ^{51}V NMR that the staggered moments are induced in a whole system by the existence of the open ends in the chains.[44]

γ-LiV_2O_5 is more conductive than α'-$Na_xV_2O_5$ but is semiconductive. The electric resistivity of γ-$Li_xV_2O_5$ measured along the *b*-axis (the linear chain direction)

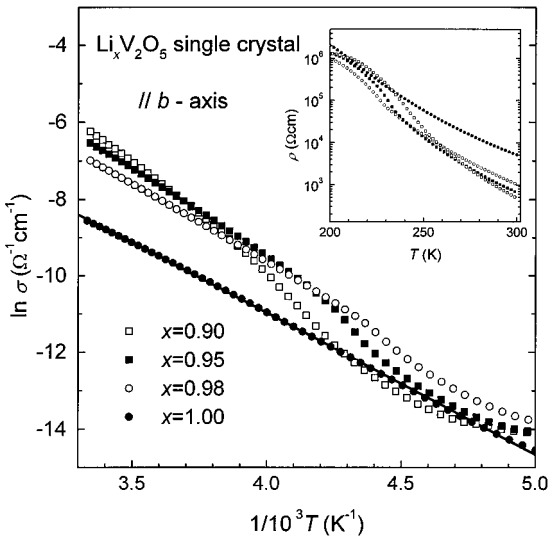

Figure 21. Logarithm of the electric resistivity versus $1/T^{-1}$ of γ-$Li_xV_2O_5$. The inset shows the resistivity of γ-$Li_xV_2O_5$ as a linear function of temperature. The resistivity is measured along *b*-axis parallel to the 1-D chains using single crystals.

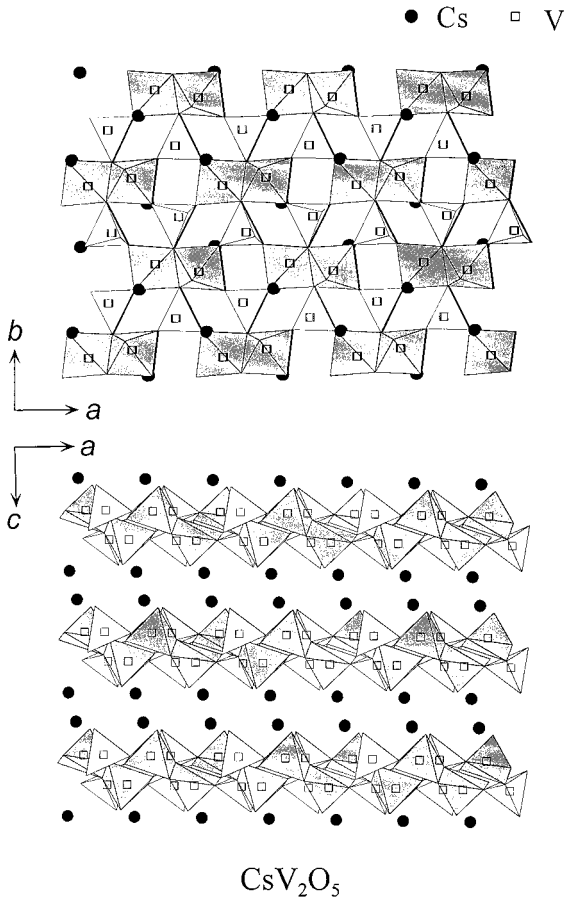

Figure 22. Schematic crystal structure of monoclinic CsV_2O_5. The VO_5 (shaded) square pyramids and the VO_4 (white) tetrahedra are occupied by V^{4+} and V^{5+} ions, respectively.

using single crystals is shown in Figure 21. The resistivity of stoichiometric γ-LiV_2O_5 shows an activation type behavior, and the energy gap was estimated to be ~0.32 eV. The resistivity of γ-$Li_xV_2O_5$ decreases with Li deficiency at 300 K but γ-$Li_xV_2O_5$ remains semiconductive. The temperature dependence of the resistivity of γ-$Li_xV_2O_5$ does not obey any activation

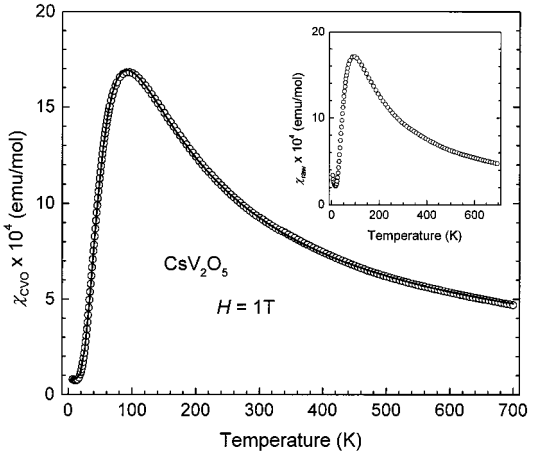

Figure 23. Temperature dependence of magnetic susceptibility of CsV_2O_5 derived by subtracting the Curie contribution from impurities. The solid line shows a fit to the equation for $S = 1/2$ Heisenberg dimer model with $J/k_B = 146$ K and $g = 1.8$. The inset shows the raw data of magnetic susceptibility.

types, as shown in Figure 21. This result suggests that the carriers are possibly doped into the 1-D linear chains, but the conducting behavior of the doped samples is not of a variable range hopping and is more complex.

CsV_2O_5 (Dimer System)

The crystal structure of CsV_2O_5 is somewhat different from those of γ-LiV_2O_5 and α'-NaV_2O_5. The structure of monoclinic CsV_2O_5 is also a layer one with cesium ions between the layers, as shown in Figure 22.[42,45] The vanadium atoms, on two distinct crystallographic sites, exhibit two types of coordination polyhedra. One type is in a square pyramid formed by five oxygens, whereas the other is tetrahedrally surrounded by four oxygens. The bond valence analysis reveals that the V sites in the VO_5 (shaded) square pyramids and the VO_4 (white) tetrahedra are occupied by V^{4+} and V^{5+} ions, respectively.[45] Two square pyramids share an edge in such a way that each terminal oxygen is in above and below the plane formed by the equatorial. These isolated double square pyramids are linked by the VO_4 tetrahedra to form the layer.

The temperature dependence of the magnetic susceptibility of CsV_2O_5 is shown in Figure 23.[42] The magnetic susceptibility has a maximum at ~90 K. The upturn of magnetic susceptibility below 20 K is considered to be due to the existence of impurities and/or free ions caused by defects. In CsV_2O_5, the magnetic $V^{4+}O_5$ square pyramids form a dimer instead of a linear chain in γ-LiV_2O_5 or α'-NaV_2O_5 and the dimers are isolated by the nonmagnetic $V^{5+}O_4$ tetrahedra, as already mentioned. The magnetic susceptibility for the $S = 1/2$ Heisenberg dimers is given as,[46]

$$\chi_{raw} = \chi_{CVO} + \chi_{imp} = \frac{Ng^2\mu_B^2}{k_BT}\frac{1}{3 + \exp\left(-\frac{2|J|}{k_BT}\right)} + \chi_o + \chi_{imp}$$

where χ_{CVO} and χ_{imp} are the contribution of magnetic susceptibility from pure CsV_2O_5 and impurities, respectively, and g and J are the powder-averaged g-factor

Table 2. Vanadate Family as Spin-gap Systems

vanadate	quantum spin system	sharing of $V^{4+}O_5$	J (K)	Δ (K)
α'-NaV_2O_5	spin-Peierls	corner	560	114
CsV_2O_5	dimer	edge	146	160
γ-LiV_2O_5	1-D zigzag chain	corner/edge	310	
CaV_2O_5	ladder	corner/edge		600
MgV_2O_5	ladder	corner/edge		17

and the exchange constant, respectively. The raw data (χ_{raw}) of magnetic susceptibility observed in CsV_2O_5 can be excellently fitted to this equation with $J/k_B = 146$ K[42] and $g = 1.8$, as shown in the solid line in Figure 23. The subtraction of χ_{imp} from χ_{raw} gives a small constant value of $\chi_0 = 8 \times 10^{-5}$ (emu/mol) below 30 K. This value is comparable to the magnetic susceptibility of the insulating phase of VO_2[47] and the ground state in the spin-Peierls compound α'-NaV_2O_5 in which spin-singlet $V^{4+}-V^{4+}$ pairs are formed. This result indicates that the ground state of CsV_2O_5 is a spin-singlet state. The spin-gap energy can be estimated from the NMR experiments to be the same order ($\Delta = 160$ K) of the exchange interaction.

Overview

All of vanadium oxides reviewed here are low-dimensional, spin-1/2 magnets that belong to various kinds of quantum-spin systems and are spin-gap systems except γ-LiV_2O_5. They are summarized in Table 2. The characteristic low-dimensional spin structures of these compounds are formed by sharing edges and/or corners of $V^{4+}O_5$ square pyramids in the manner that each apical oxygen is located in the opposite side from the basal plane in the edge-sharing pyramids and is in the same side in the corner-sharing pyramids. α'-NaV_2O_5 includes 1-D chains formed by only corner-sharing $V^{4+}O_5$ square pyramids, whereas CsV_2O_5 includes dimers formed by only edge-sharing $V^{4+}O_5$ square pyramids. The observed exchange integral J of α'-NaV_2O_5 is much larger than that of CsV_2O_5. This means that the exchange interaction is much stronger in the corner-sharing $V^{4+}O_5$ square pyramids than in the edge-sharing pyramids. γ-LiV_2O_5 has 1-D zigzag chains in which the spins interact through both the edges and the corners of $V^{4+}O_5$ square pyramids. It should be noticed that the exchange integral of 310 K observed in γ-LiV_2O_5 is very close to the difference of J between α'-NaV_2O_5 and CsV_2O_5. The exchange integrals of CaV_2O_5 and MgV_2O_5 cannot be estimated from the temperature dependence of magnetic susceptibility because of the spin-ladder structure. CaV_2O_5 and MgV_2O_5 are spin-ladder systems with spin gaps and the observed energy gap is much larger in CaV_2O_5 than in MgV_2O_5. This difference may be related to the difference of the local structure; that is, the difference of the exchange interaction.

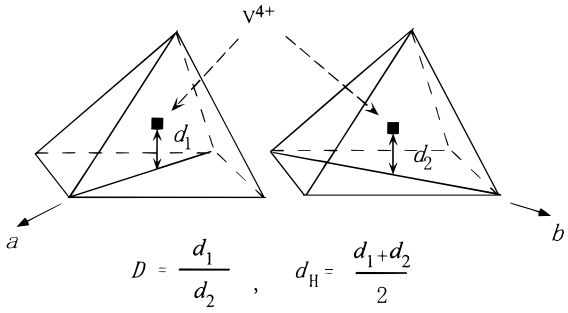

Figure 24. The definition of the distortion (D) of $V^{4+}O_5$ square pyramid and the distance (d_H) of the V^{4+} ion from the basal plane.

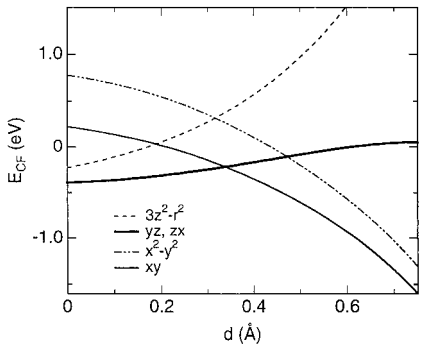

Figure 25. Crystal field levels of a V^{4+} ion in a regular VO_5 pyramid with the equi-distance of $d_{V-O} = 1.9$ Å, calculated from a simple point charge model, as a function of the distance of the V^{4+} ion from the basal plane (ref 48).

The various local, structural parameters derived from the crystal structure at room temperature are summarized in Table 3. In all compounds, the $V^{4+}O_5$ square pyramids are distorted and the basal plane is not flat. The parameter D in Table 3, which shows a degree of distortion of the basal plane, is expressed as the ratio of the distance (d_1) of V^{4+} ions from the center of diagonal line along the a-axis to that (d_2) along the b-axis, as shown in Figure 24. The parameter d_H (distance of the V^{4+} ions from the basal plane) in Table 3 is the average of d_1 and d_2. The basal plane of the $V^{4+}O_5$ square pyramid is distorted in γ-LiV_2O_5 and CsV_2O_5, whereas it is rather flat in α'-NaV_2O_5, CaV_2O_5, and MgV_2O_5. Ohama et al.[48] calculated the crystal field splitting of a V^{4+} ion in a regular VO_5 pyramid with the equidistance of $d_{V-O} = 1.9$ Å from a simple point charge model. The crystal field levels obtained are shown in Figure 25 as a function of the distance of the V^{4+} ions from the basal plane. The ground state of d levels changes from the doublet d_{yz}, d_{zx} to the singlet d_{xy} upon increasing the shift of the V^{4+} ion from the basal plane. The results indicate that the ground state is d_{xy} in this vanadate family, because the averaged distance of V^{4+} ion from the basal plane is scattered around 0.6−0.7 Å in all compounds, although the real

Table 3. Structural Parameters[a]

	∥chain			⊥chain			edge		
vanadate	d_{V-O}	θ_{O-V-O}	d_{V-V}	d_{V-O}	θ_{O-V-O}	d_{V-V}	d_{V-V}	d_H	D
α'-NaV_2O_5	1.962	23.06	3.611					0.7231	1.134
CsV_2O_5							3.073	0.5771	1.684
γ-LiV_2O_5	1.960	23.06	3.004				3.004	0.6533	1.424
CaV_2O_5	1.949	22.36	3.605	1.905	23.55	3.492	3.025	0.6564	1.298
MgV_2O_5	1.957	19.43	3.692	1.971	31.22	3.372	2.983	0.6712	0.942

[a] Distances (d) are in Å and Angles (θ) are in degrees.

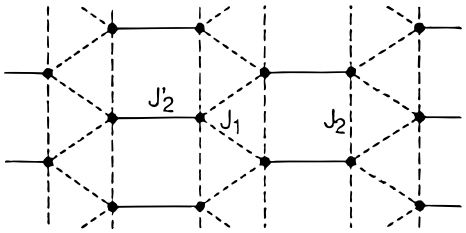

Figure 26. Schematic representation of the frustrated coupled-ladder system.

Table 4. Estimated Exchange Integrals in Kelvin[a]

vanadate	J_1	J_2	J'_2	J_2/J_1	J'_2/J_1
α'-NaV_2O_5		530			
CsV_2O_5	146				
γ-LiV_2O_5[b]	183[b]	568[b]		3.1[b]	
CaV_2O_5	170	587	730	3.5	4.3
MgV_2O_5	201	565	511	2.8	2.5

[a] Reference 50. [b] Present work.

VO_5 pyramid is not a regular VO_5 pyramid with equi-d_{V-O} and is distorted. Actually, the observed anisotropy of the NMR and the electric field gradient (EFG) indicates that the d_{xy}-like orbital is occupied in α'-NaV_2O_5 and CaV_2O_5.[48]

Marini and Khomskii[36] discussed a large spin gap in CaV_2O_5 from the formation of tightly bound dimers caused by V ions shift and corresponding orbital ordering. In their model, a *d*-electron occupies the *zx*-like orbital and V ions form dimers along the rungs. The out-of-plane position of V ions leads to an extra contribution to the exchange that is due not only to π- but also to σ-overlap. The strong exchange interaction of the order of the spin gap is due to σ-overlap. This model seems to explain a large spin gap or strong exchange interaction but the occupied *d*-orbital (*zx*-like orbital), which is essential in their model, is inconsistent with the NMR results.

Normand et al.[49] studied the theoretical magnetic phase diagram of the frustrated coupled-ladder structure and Millet et al.[50] discussed the vanadate family according to the analysis of the model performed by Normand et al.[49] Figure 26 shows the schematic representation of the frustrated coupled-ladder system. Millet et al.[50] estimated the exchange integrals of CaV_2O_5 and MgV_2O_5 based on the structural and magnetic information, assuming that these depend only on the local geometry of the bonds. The results are shown in Table 4 together with our estimation for γ-LiV_2O_5, where the exchange integrals of CsV_2O_5 and α'-NaV_2O_5 are used as a measure to estimate J_1 and J_2 (or J'_2) in other members, respectively. According to their explanation, the ratio $J'_2/J_1 = 4.3$ clearly puts CaV_2O_5 in the ladder limit with a large gap, whereas $J'_2/J_1 = 2.5$ with $J_2/J_1 = 2.8$ puts MgV_2O_5 very close to the helical ordered-hence gapless-phase and the system is thus expected to have a very small gap.

These vanadate family members belong to various kinds of quantum-spin systems and have provided a stage where various quantum spin phenomena can be investigated systematically, similar to the cuprates. For further investigation it is necessary to grow single crystals that have enough size to measure anisotropic properties. Large crystals of α'-NaV_2O_5 and γ-LiV_2O_5 have been successfully grown[8] but others have not been yet. The information derived from the systematic study will serve as fundamental data for materials design or for developing new materials. At present, the author has no idea of applications of these quantum-spin systems, but suggests that quantum spin phenomena might receive attention in connection with potential devices called "spinics" (which is a parody on "electronics") in the next generation.

References

(1) For reviews see: Mott, N. F. *Metal−Insulator Transition*; Taylor and Francis; London, 1974.
(2) Hase, M.; Terasaki, I.; Uchinokura, K. *Phys. Rev. Lett.* **1993**, *70*, 3651.
(3) Ishida, K.; Kitaoka, Y.; Asayama, K.; Azuma, M.; Hiroi, Z.; Takano, M. *J. Phys. Soc. Jpn.* **1994**, *63*, 3222.
(4) Taniguchi, S.; Nishikawa, T.; Yasui, Y.; Kobayashi, Y.; Sato, M.; Nishioka, T.; Kontani, M.; Sano, K. *J. Phys. Soc. Jpn.* **1995**, *64*, 2758.
(5) Carpy, A.; Galy, J. *Acta Crystallogr. Sect.* **1975**, *B31*, 1481.
(6) Isobe, M.; Ueda, Y. *J. Phys. Soc. Jpn.* **1996**, *65*, 1178.
(7) Bonner, J. C.; Fisher, M. E. *Phys. Rev.* **1964**, *135*, A640; Hatfield, W. E. *J. Appl. Phys.* **1981**, *52*, 1985.
(8) Isobe, M.; Kagami, C.; Ueda, Y. *J. Crystal Growth* **1997**, *181*, 314.
(9) Bray, J. W.; Hart, H. R. Jr.; Interrante, L. V.; Jacobs, I. S.; Kasper, J. S.; Watkins, G. D.; Wei, S. H.; Bonner, J. C. *Phys. Rev. Lett.* **1975**, *35*, 744.
(10) Jacobs, I. S.; Bray, J. W.; Hart, H. R. Jr.; Interrante, L. V.; Kasper, J. S.; Watkins, G. D.; Prober, D. E.; Bonner, J. C. *Phys. Rev.* **1976**, *B14*, 3036.
(11) Huizinga, S.; Kommandeur, J.; Sawatzky, G. A.; Thole, B. T.; Kopinga, K.; de Jonge, W. J. M.; Roos, J. *Phys. Rev.* **1979**, *B19*, 4723.
(12) Jacobsen, C. S.; Pedersen, H. J.; Mortensen, K.; Bechgaard, K. *J. Phys. C.; Solid State Phys.* **1980**, *13*, 3411.
(13) Ohama, T.; Isobe, M.; Yasuoka, H.; Ueda, Y. *J. Phys. Soc. Jpn.* **1997**, *66*, 545.
(14) Fujii, Y.; Nakao, H.; Yoshihama, T.; Nishi, M.; Kakurai, K.; Isobe, M.; Ueda, Y. *J. Phys. Soc. Jpn.* **1997**, *66*, 326.
(15) Yoshihama, T.; Nishi, M.; Nakajima, K.; Kakurai, K.; Fujii, Y.; Isobe, M.; Ueda, Y. *Physica B* **1997**, *234−236*, 539.
(16) Kamimura, O.; Terauchi, M.; Tanaka, M.; Fujita, O.; Akimitsu, J. *J. Phys. Soc. Jpn.* **1994**, *63*, 2467.
(17) Pouget, J. P.; Regnault, L. P.; Ain, M.; Hennion, B.; Renard, J. P.; Veillet, P.; Dhalenne, G.; Revcolevschi, A. *Phys. Rev. Lett.* **1994**, *72*, 4037.
(18) Hirota, K.; Cox, D. E.; Lorenzo, J. E.; Shirane, G.; Tranquada, J. M.; Hase, M.; Uchinokura, K.; Kojima, H.; Shibuya, Y.; Tanaka, I. *Phys. Rev. Lett.* **1994**, *73*, 736.
(19) Vasil′ev, A. N.; Smirnov, A. I.; Isobe, M.; Ueda, Y. *Phys. Rev.* **1997**, *B56*, 5065.
(20) Bray, J. W.; Interrante, L. V.; Jacobs, I. S.; Bonner, J. C. *Extended Linear Chain Compounds*; Miller, J. S., Ed.; Plenum: New York and London, 1983, *3*, 353.
(21) Ohama, T.; Isobe, M.; Yasuoka, H.; Ueda, Y., submitted for publication in *Phys. Rev. Lett.*
(22) Vasil'ev, A. N.; Pryadun, V. V.; Khomskii, D. I.; Dhalenne, G.; Revcolevschi, A.; Isobe, M.; Ueda, Y. *Phys. Rev. Lett.* **1998**, *81*, 1949.
(23) Sekine, Y.; Takeshita, Nao.; Môri, N.; Isobe, M.; Ueda, Y., submitted for publication in *J. Phys. Soc. Jpn.*
(24) von Schnering, H. G.; Grin, Yu.; Kaupp, M.; Somer, M.; Kremer, R. K.; Jepsen, O.; Chatterji, T.; Weiden, M. *Z. Kristallogr. New Crystal Structure*, **1998**, 213, 246. Meetsma, A., et al., submitted for publication in *Acta Crystallogr.*
(25) Isobe, M.; Ueda, Y. *J. Alloys Compd.* **1997**, *262−263*, 180.
(26) Hase, M.; Koide, N.; Manabe, K.; Sasago, Y.; Uchinokura, K.; Sawa, A. *Physica B* **1995**, *215*, 164.
(27) Lussier, J.-D.; Coad, S. M.; McMorrow, D. F.; Paul, D. McK. *J. Phys.; Condens. Matter* **1995**, *7*, L325.
(28) Renard, J. P. K.; Dang, Le; Veillet, P.; Dhalenne, G.; Revcolevschi, A.; Regnault, L. P. *Europhys. Lett.* **1995**, *30*, 475.
(29) Azuma, M.; Hiroi, Z.; Takano, M.; Ishida, K.; Kitaoka, Y. *Phys. Rev. Lett.* **1994**, *73*, 3463.
(30) Sigrist, M.; Furusaki, A. *J. Phys. Soc. Jpn.* **1996**, *65*, 2385.
(31) Iino, Y.; Imada, M. *J. Phys. Soc. Jpn.* **1996**, *65*, 3728.
(32) Bouloux, J. C.; Galy, J. *J. Solid State Chem.* **1976**, *16*, 385.
(33) Dagotto, E.; Rice, T. M. *Science* **1996**, *271*, 618.
(34) Iwase, H.; Isobe, M.; Ueda, Y.; Yasuoka, H. *J. Phys. Soc. Jpn.* **1996**, *65*, 2397.
(35) Troyer, M.; Tsunetsugu, H.; Würtz, D. *Phys. Rev.* **1994**, *B50*, 13515.

(36) Onoda, M.; Nishiguchi, N. *J. Solid State Chem.* **1996**, *127*, 359, Marini, S.; Khomskii, D. I., unpublished results.
(37) Bouloux, J. C.; Milosevic, I.; Galy, J. *J. Solid State Chem.* **1976**, *16*, 393.
(38) Isobe, M.; Ueda, Y.; Takizawa, K.; Goto, T. *J. Phys. Soc. Jpn.* **1998**, *67*, 755.
(39) Uemura, Y. J., et al., private communication.
(40) Mori, T. et al., manuscript in preparation.
(41) Anderson, D. N.; Willett, R. D. *Acta Crystallogr. Sect.* **1971**, *B27*, 1476.
(42) Isobe, M.; Ueda, Y. *J. Phys. Soc. Jpn.* **1996**, *65*, 3142.
(43) Fujiwara, N.; Yasuoka, H.; Isobe, M.; Ueda, Y. *Phys. Rev.* **1997**, *55*, R11945.
(44) Fujiwara, N.; Yasuoka, H.; Isobe, M.; Ueda, Y., submitted for publication in *Phys. Rev.*
(45) Waltersson, K.; Forslund, B. *Acta Crystallogr. Sect.* **1977**, *B33*, 789.
(46) Carlin, R. L. *Magnetochemistry*; Springer-Verlag: Berlin, 1986; Vol. 5, p 75.
(47) For reviews see: Goodenough, J. B. *Progress in Solid State Chemistry*; Pergamon: New York, 1971, 5, 145; Mott, N. F. *Metal−Insulator Transition*; Taylor and Francis: London, 1974.
(48) Ohama, T.; Yasuoka, H.; Isobe, M.; Ueda, Y. *J Phys. Soc. Jpn.* **1997**, *66*, 3008.
(49) Normand, B.; Penc, K.; Albrecht, M.; Mila, F. *Phys. Rev.* **1997**, *B56*, R5736.
(50) Millet, P.; Satto, C.; Bonvoisin, J.; Normand, B.; Penc, K.; Albrecht, M.; Mila, F.; *Phys. Rev.* **1998**, *B57*, 5005.

CM980215W